Environmental Science & Technology

Article

Cite This: Environ. Sci. Technol. 2019, 53, 13042−13052

pubs.acs.org/est

Microenvironmental Interplay Predominated by Beneficial *Aspergillus* Abates Fungal Pathogen Incidence in Paddy Environment

Xiaoyan Fan,[†,▽] Haruna Matsumoto,[†,▽] Yue Wang,[†] Yang Hu,[§] Yufei Liu,[‡,▽] Hongda Fang,[∥] Bartosz Nitkiewicz,[⊥] Sharon Yu Ling Lau,[#] Qiangwei Wang,[†] Hua Fang,[†] and Mengcen Wang*[,†]

[†]Ministry of Agriculture Key Laboratory of Molecular Biology of Crop Pathogens and Insects, Institute of Pesticide and Environmental Toxicology and [‡]College of Biosystems Engineering and Food Science, Zhejiang University, Hangzhou 310058, China

[§]Zhejiang Provincial Key Laboratory of Biological and Chemical Utilization of Forest Resources, Zhejiang Academy of Forestry, Hangzhou 310058, Zhejiang, China

[∥]College of Plant Protection, Hunan Agricultural University, Changsha 410128, China

[⊥]Department of Biochemistry, Faculty of Biology and Biotechnology, University of Warmia and Mazury, Oczapowskiego 1A, 10-719 Olsztyn, Poland

[#]Sarawak Tropical Peat Research Institute, 94300 Kota Samarahan, Sarawak, Malaysia

Supporting Information

ABSTRACT: Rice fungal pathogens, responsible for severe rice yield loss and biotoxin contamination, cause increasing concerns on environmental safety and public health. In the paddy environment, we observed that the asymptomatic rice phyllosphere microenvironment was dominated by an indigenous fungus, *Aspergillus cvjetkovicii*, which positively correlated with alleviated incidence of *Magnaporthe oryzae*, one of the most aggressive plant pathogens. Through the comparative metabolic profiling for the rice phyllosphere microenvironment, two metabolites were assigned as exclusively enriched metabolic markers in the asymptomatic phyllosphere and increased remarkably in a population-dependent manner with *A. cvjetkovicii*. These two metabolites evidenced to be produced by *A. cvjetkovicii* in either a phyllosphere microenvironment or artificial media were purified and identified as 2(3*H*)-benzofuranone and azulene, respectively, by gas chromatography coupled to triple quadrupole mass spectrometry and nuclear magnetic resonance analyses. Combining with bioassay analysis in vivo and in vitro, we found that 2(3*H*)-benzofuranone and azulene exerted dissimilar actions at the stage of infection-related development of *M. oryzae*. *A. cvjetkovicii* produced 2(3*H*)-benzofuranone at the early stage to suppress *MoPer1* gene expression, leading to inhibited mycelial growth, while azulene produced lately was involved in blocking of appressorium formation by downregulation of *MgRac1*. More profoundly, the microenvironmental interplay dominated by *A. cvjetkovicii* significantly blocked *M. oryzae* epidemics in the paddy environment from 54.7 to 68.5% ($p < 0.05$). Our study first demonstrated implication of the microenvironmental interplay dominated by indigenous and beneficial fungus to ecological balance and safety of the paddy environment.

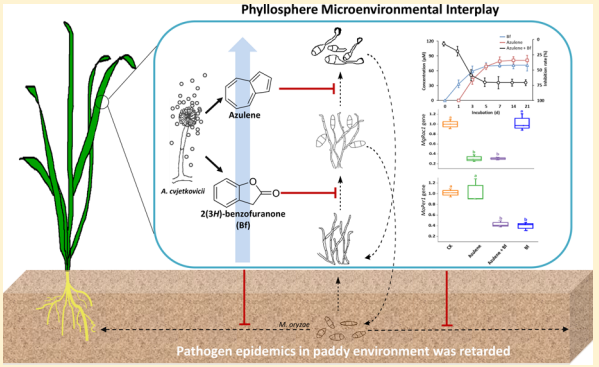

INTRODUCTION

Paddy environment, as the largest and representative agricultural environment in the world, functions as an important origin to produce foods for an increasing population and forage for livestock, especially in Asian countries.[1−3] However, it is remarkable that dispersion and transmission of rice fungal pathogens in the paddy environment not only causes severe loss of rice yield[4] but also leads to an increasing global concern on biotoxin contamination on agricultural products and even the relevant environments.[5−8]

In the past decades, *Magnaporthe oryzae*, the causal agent of plant blast disease, has arisen as one of the most aggressive fungal pathogens in the global agricultural environment, especially in the paddy environment.[4,6] It was reported that the losses of grain on accounts of *M. oryzae* could be 10−30%.[9] The major primary infection source of *M. oryzae* in the paddy

Received: July 31, 2019
Revised: October 12, 2019
Accepted: October 20, 2019
Published: October 20, 2019

DOI: 10.1021/acs.est.9b04616
Environ. Sci. Technol. 2019, 53, 13042−13052

environment originates from vegetative mycelia and conidia, which could overwinter in seeds, plant residues, and even the paddy soils, and can be disseminated by wind and rain throughout the paddy environment.[10−12] Due to the constant global warming and climate change, epidemic, outbreak, and incidence of rice blast in the paddy environment were aggravated recently.[13] It is estimated that the each year's loss of grain destroyed by *M. oryzae* could feed 60 million people.[14] *M. oryzae* is capable of invading rice in the whole growth period and producing lesions on all organs of the rice plant.[14] Along with occurrence of symptoms such as leaf blast, neck blast, and panicle blast,[15,16] this fungal pathogen produces an array of biotoxins including pyricuol, tenuazonic acid, cercosporin, etc.[6,17,18] In addition to breeding of resistant varieties, an assortment of chemical pesticide-dominated plant disease management strategies have been developed to control *M. oryzae*, but the low efficacy, the enhancement of pathogen drug resistance, and also the emerging organic contamination become increasingly non-negligible,[19] attributed to the fact that physiological variability responsible for high plasticity of this fungus enhances their survival in different and even hostile environments.[20] Hence, environmental and ecological strategies are deemed to be promising approaches to address this issue, irrespective of the fact that little is known in the case of *M. oryzae*.

Previous reports have provided direct evidences about the close correlation between plant growth and its alterative microenvironment[21,22] in which abundant and diverse indigenous microbes live in one adjacent environment and interact with each other, as described to be a critical element in determining plant development and health.[23,24] Particularly, the metabolic interactions between beneficial microbe and invasive pathogen play a pivotal role in preservation of microecological balance.[25] In terms of the microenvironment (microecological environment of an organism, considered as a distinct part in comparison with its surrounding environment), previous researches were mainly focus on interplay between rhizosphere microbiome and plant.[26−30] However, up to date, little is known regarding the indigenous key microbes in above-ground part of paddy, especially in the rice phyllosphere, and associated metabolic interaction to repel invasive fungal pathogens.[31]

Interestingly, during a large-scale screening of phyllospheric indigenous microbes,[32] a pigmented and morphology-analogous fungal isolate was exclusively observed from the asymptomatic rice phyllosphere, while this fungus was absent in the adjacent diseased ones. In in vitro and in vivo tests, this fungus exerted potent antagonistic effect on *M. oryzae* and promoting effect on rice. Thus, we hypothesized that this indigenous fungus in the rice phyllosphere might maintain the microenvironmental equilibrium through a metabolic interplay against *M. oryzae* invasion.[25]

To clarify our hypothesis, we identified this fungus using morphological and internal transcribed spacer (ITS) sequence-based phylogenetic analyses. From this indigenous fungus, two extracellular small molecules were further isolated, purified, and identified to participate in the active metabolic interplay against *M. oryzae* and maintain the fitness consequence of the host microenvironment.[33−35] Morphological alteration of *M. oryzae* upon exposure to these molecules together with qRT-PCR analysis revealed the possible targeted physiological process by these active small molecules derived from this indigenous fungus. Moreover, it was also evidenced that the microenvironmental interplay plays a pivotal role in blocking epidemic cycles of *M. oryzae* in the paddy environment. Our work provides insights into the ecological implication of microenvironmental interplay of the key indigenous fungus to protect rice from invasive pathogen and, more importantly, sheds light on the management of *M. oryzae* incidence and the relevant biotoxin contamination in the paddy environment.

MATERIALS AND METHODS

Paddy Field Sites and Sampling. Field sampling was carried out in Hangzhou, Jinhua, and Jiaxing, three typical rice production regions in Zhejiang province, where the diverse rice cultivars (nonresistant against *M. oryzae*) including Xiushui 09, Zhongjiazao 17, and Yongyou 15, respectively, were cultivated. In each sampling site, the paddy fields without *M. oryzae* incidence at the stage of rice tillering were selected for collection of asymptomatic phyllosphere samples, while those with *M. oryzae* incidence were deemed as symptomatic samples. Twenty asymptomatic and twenty symptomatic phyllosphere samples (2.0 kg per sample) were collected from the relevant leaves using a complete randomized block design for each corresponding field. Each sample was divided quarterly and stored in a freezer at −80 °C for further experiments.

Microbial Strains, Media, and Culture Conditions. *M. oryzae* was previously isolated and identified from the diseased rice leaves, in Zhejiang province, China. As the growth condition for *M. oryzae* and other microbial strains in this study, Luria broth (LB), nutrition broth (NB), modified Winogradsky (MW), potato dextrose (PD), and complete medium (CM) were employed with or without supplementation of agar (1.5%) according to each specific experiment described below. For routine cultures, *M. oryzae* and other fungal isolates were incubated at 25 °C in the dark.

Screening of the Indigenous Microbes against *M. oryzae* from Rice Phyllosphere. The leave samples were thoroughly washed to remove the airborne counterparts using sterile water, and then each sample was weighed 10 g. After being transferred into a sterilized mortar, it was ground with 20 mL of sterilized distilled water premixed with quartz sand. The resulting suspension was left to stand for 15 min from which 1 mL of the supernatant was used for a serial dilution and as an inoculant. CM agar (CMA) was used as a culture medium onto which each inoculant was spread evenly with a glass spreader and incubated for 5 days at 25 °C in the dark. Subsequently, all culturable and distinguishable fungal colonies after purification were isolated, counted, and assessed their antagonistic activity on *M. oryzae*.

The antagonistic efficacy in vitro of the isolates was tested against *M. oryzae* by a dual-culture experiment. One 5 mm agar plug was cut from the edge of actively growing colony of *M. oryzae* on the CMA plate and then placed on the center of a new fresh CMA plate. Then, two mycelial plugs of each fungal isolate were symmetrically placed onto the above pre-inoculated plate, at an equidistant distance of 2 cm from the center. The portion of non-inoculation of the isolates on the plate was served as the control. Incubation was carried out at 25 °C in the dark for 5 days and subjected to evaluation of the inhibitory effect by measuring the diameter of the mycelia and calculating the percentage of radial growth inhibition using the following formula: $(S_c - S_t)/(S_c - d) \times 100$, where S_c and S_t (mm) represent the length of the mycelial growth in control

DOI: 10.1021/acs.est.9b04616
Environ. Sci. Technol. 2019, 53, 13042−13052

and treatment, respectively, and d (mm) is the diameter of the agar plug.[36]

Identification and Quantification of the Key Phyllosphere Fungal Isolates against *M. oryzae*. Morphological and phylogenetic analyses were carried out for identification of the fungal isolates possessing significant antagonistic activity against *M. oryzae*. The mycelia and conidia of the fungal isolates were respectively harvested after 7 days of incubation on the CMA plate at 25 °C in the dark and subsequently observed under the light microscope (Nikon E100, Japan).

For the molecular phylogenetic analyses, the fresh mycelia of the isolates were collected respectively for extraction of genomic DNA using a Mini fungus genomic DNA Extraction kit (Takara Bio Inc.) according to the manufacturer's instructions. DNA purity and concentration were measured using a NanoDrop ND-100 spectrophotometer (NanoDrop Technologies, Rockland, DE, USA). Then, the ITS region was amplified with the universal primers of ITS1 and ITS4 (Table S4), and *CaM* gene was amplified with primers C5 and C6 (Table S4) using the following PCR procedure: 97 °C for 5 min, subsequently 30 cycles at 97 °C for 30 s, annealing at 56 °C for 45 sand at 72 °C for 45 s, and a final extension at 72 °C for 10 min. All the DNA sequences of the fungal isolates were compared for similarity with publicly available reference sequences from the NCBI nucleotide database; then, the phylogenetic trees were constructed using neighbor joining by MEGA7.

To quantify the abundance of the key phyllosphere *M. oryzae*-antagonistic fungal isolates, the specific primers (21F/21R) based on *CaM* were designed using Primer Premier 6.0 (Table S4). The qPCR was performed following the program described in previous reports.[37,38]

Characteristics and Variation of the Metabolic Profiles between Asymptomatic and Symptomatic Phyllosphere. To analyze the differential metabolic profiles of the rice phyllosphere, the asymptomatic and symptomatic rice leaves collected above were thoroughly washed and spiked with the same concentrations of spirodiclofen (an artificial pesticide that is not used in the paddy environment and also cannot be produced by either rice or microbiota) as the internal standard. After homogenizing evenly with liquid nitrogen, 2 g of each resulting homogenates was supplemented with 10 mL of methanol (MeOH)−ultrapure water (1:1, v/v) and shaken on an automatic horizontal shaker at 180 rpm for 30 min, following by sonication for 30 min. After centrifugation at 4000 rpm for 30 min, the aliquot of supernatant was evaporated to remove MeOH under low pressure and the resulting solutions were then exhaustively extracted twice with ethyl acetate (EtOAc) after adjusting to pH 3.5. Finally, the EtOAc extracts dried with anhydrous sodium sulfate were concentrated to remove the organic solvent, resuspended in EtOAc, and filtered through a 0.22 μm filter for further gas chromatography coupled to triple quadrupole mass spectrometry (GC-QqQ-MS/MS) analysis.[32]

GC-QqQ-MS/MS (Agilent 7000C Technology, CA, USA) analysis was carried out being equipped with a capillary column (Agilent DB-1, 30 m × 0.25 mm inside diameter (i.d.) with 0.25 μm film thickness). High-purity helium (99.999%) was used as carried gas with a flow rate of 3 mL min^{-1}, and the collision gas nitrogen (99.999%) was at a rate of 1.5 mL min^{-1}. The initial oven temperature was held at 60 °C for 2 min and then increased to 180 °C at a rate of 15 °C min^{-1}, stable for 2 min, and the subsequent temperature was programmed from 180 to 250 °C at a rate of 30 °C min^{-1} with a final hold for 5 min. The temperature of injector, transfer line, and ion source were 250, 280 and 230 °C, respectively. The mass spectrometer was conducted in the electron ionization mode with 70 eV ionization energy scanned from m/z 40 to 450 with a 3.5 s scan time delay. The injection was done at the analyte volume of 1 μL under the splitless mode.

Production and Isolation of the Metabolites Produced by *A. cvjetkovicii*. For production analysis of the metabolites in *A. cvjetkovicii*, large-scale culture of *A. cvjetkovicii* was conducted in 3000 mL of CM. Two mycelial plugs of *A. cvjetkovicii* were cut from the actively growing margin of 7 day-old mycelia and inoculated in each 250 mL erlenmeyer flask containing 100 mL of CM at 150 rpm at 25 °C in the dark for 7 days. The culture supernatant was collected, adjusted pH to 3.5 after centrifugation at 12,000 rpm for 10 min, and then subjected to extraction with EtOAc as described in the above method.

The crude extracts dissolved in EtOAc were obtained for further separation by chromatography on a column (4.5 cm i.d. × 40 cm length) packed with 50 g of 200 mesh silica gel. Subsequently, stepwise gradient elution with 5 to 95% EtOAc in *n*-hexane was performed to separate the extracts into 12 fractions with 20 mL collection per fraction possessing different polarities, each fraction of which was then concentrated for further bioassay and metabolic profiling.

Bioassay of *A. cvjetkovicii* and its Derived Metabolites in Vitro and in Vivo. The paper disk method was conducted in vitro to estimate the antifungal activity of each separated fraction dissolved in EtOAc. The sterile filter paper disk (5 mm in diameter) was filled with crude extracts of *A. cvjetkovicii* (each disk contained one fraction) and then dried up and subsequently placed on the surface of a 9 mm CMA plate, at a 3 mm distance from the center agar plugs containing mycelia of *M. oryzae*. The paper disk loaded with EtOAc was placed on the other equidistant side used as the control. The inhibitory effect was measured after incubation for 5 days at 25 °C in the dark. Each experiment was repeated three times.

For the bioassay in vivo, rice plants were cultivated under the conditions described previously,[39] different concentrations of conidia suspensions (1×10^5 conidia mL^{-1} with 0.02% Tween 80) were prepared from *A. cvjetkovicii* for spraying the phyllosphere, and sterile water was used as the control. The *M. oryzae* agar plugs were placed on the phyllosphere at three equidistant pre-injured points and were then subjected to incubation at 22 °C for the first 48 h in darkness. Then, they were transferred into another incubator for subsequent culture under alternating 12 h light and 12 h dark at 25 °C with the same conditions. After 5 days of inoculation, the disease relative lesion area (RLA) of each treatment was statistically visualized and calculated using the Otsu method for evaluation of the disease incidence.[40]

Identification and Quantification of the Active Metabolites from *A. cvjetkovicii*. The active fractions were dissolved in EtOAc at 1000 mg L^{-1} and diluted into a series of concentrations containing spirodiclofen as an internal standard for metabolic profiling by GC-QqQ-MS/MS analysis under the same condition as mentioned above in which two putative bioactive metabolites were detected at t_R of 4.28 and 5.27 min. Quantification was carried out using the multiple reaction monitoring (MRM) mode (Table S5), and data acquisition and processing were performed using the Agilent 7000C MassHunter.[41]

DOI: 10.1021/acs.est.9b04616
Environ. Sci. Technol. 2019, 53, 13042−13052

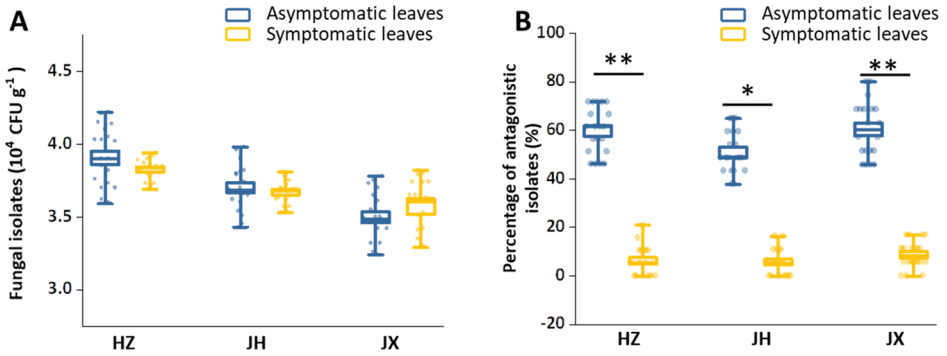

Figure 1. Comparison of (A) culturable microbial isolates and (B) antagonistic isolates in the rice phyllosphere samples collected from Hangzhou (HZ), Jinhua (JH), and Jiaxing (JX). Values are means ± standard deviations (shown by error bars) (each sample contains 20 replicates, $n = 20$). *$p < 0.05$; **$p < 0.01$.

The metabolites 1 and 2 were further subjected to structural analysis through normal nuclear magnetic resonance (NMR) spectra running on a Bruker DMX 500 instrument using DMSO-d_6 and acetone-d_6 as solvents, respectively. ^{1}H NMR and ^{13}C NMR spectroscopies were conducted to elucidate the chemical structure of these two metabolites.

Production Dynamics and Inhibitory Effect of the Active Metabolites in *A. cvjetkovicii*. Dynamics of production of two active metabolites by *A. cvjetkovicii* in CM was analyzed below. The fresh mycelia of *A. cvjetkovicii* were cultured in the shake flask containing CM at 150 rpm at 25 °C in the dark and were sampled at 0, 1, 3, 5, 7, 14, and 21 days.

The culture filtrate was extracted with EtOAc (1:1, v/v) after adjusting to pH 3.5, from each of which 1 μL was injected into the GC-QqQ-MS/MS for quantification of metabolites 1 and 2. The remaining portion was simultaneously subjected to bioassay using the paper disk method mentioned above. The subsequent correlation analyses were performed using SPSS (version 20.0).

Quantification of Gene Expression by qRT-PCR. Quantitative real-time PCR (qRT-PCR) analysis was performed to examine the expression of mycelial growth- and appressoria formation-related genes of *M. oryzae* described previously, treated with 2(3*H*)-benzofuranone and azulene. Mycelia of each treatment were harvested for RNA extraction and were subjected to reverse transcription using a PrimerScript RT reagent kit (TaKaRa Biotechnology, Japan). The qRT-PCR was conducted on the ABI 7500 real-time PCR system (Bioer Technology, Shanghai, China) according to the manufacturer's instructions. The *MoPer1* and *MgRac1* genes were amplified from the cDNA by following this procedure: 95 °C for 5 min and 40 cycles at 95 °C for 10 s, 58 °C for 30 s, and 72 °C for 30 s. Primers (MAC1F/MAC1R and MgRac1F/MgRac1R, Table S4) were used in amplifying *MoPer1* and *MgRac1* genes, respectively, and *ACTIN* gene as the internal standard was amplified with the primers ActinF and ActinR (Table S4) for normalization. Relative gene expression was analyzed based on the $2^{-\Delta\Delta Ct}$ method.[42] The experiment was repeated three times with three biological replicates each time.

Environmental Effect of the Microenvironmental Interplay on *M. oryzae* Epidemics. A large scale of field survey was carried out for observation of initial *M. oryzae* incidence in Xiaoshan, Hangzhou from which 15 fields with the same disease index at the early stage were selected and randomly divided into three groups (5 fields per group). Two groups were subjected to phyllosphere application (foliar application) of *A. cvjetkovicii* (1×10^5 conidia mL^{-1} with 0.02% Tween 80) and the mixture of derived active metabolites (1:1, 100 μM), and the remained group was used as the control. At the late tillering stage and post-harvest stage, the aerial samples collected by conidia auto samplers (Burkard Scientific) and paddy soil samples of each field were evaluated by comparing the abundance of *M. oryzae* for the relevant epidemics of *M. oryzae* at active and overwintering stages in the paddy environment. Soil samples (1 kg per field) mixed with reverse osmosis (RO) water was thoroughly homogenized and then filtrated using four layers of sterile gauze. The resulting filtrates were passed through a filter paper with a pore of 80−120 μm and followed by a filter paper with a pore of 1−3 μm. The resulting precipitate-attached filters were recovered for extraction of DNA. To quantify the abundance of *M. oryzae* in paddy air or soil, the total DNA was extracted from the soil precipitates or conidia-attached polyester films with the FastDNA SPIN Kit for soil (MP Biomedicals, USA) following the manufacturer's protocol, the specific primers (MHP1F/MHP1R, Table S4) and TaqMan probe (Table S4); and qPCR for quantification of *MHP1*, a specific marker gene of *M. oryzae*, was performed per the program described previously.[43,44]

Statistical Analyses. Statistical analyses were performed using ANOVA and Student *t*-test analysis. All significant differences between treatments were evaluated and calculated using the statistical program package SPSS (version 20.0).

Quality Assurance and Quality Control. The GC-QqQ-MS/MS quantification of 2(3*H*)-benzofuranone and azulene was validated for the limit of detection, limit of quantification, and recovery. The limit of detection was determined by considering a signal-to-noise ratio of 3, and the limit of quantification was determined by considering a signal-to-noise ratio of 10. Recovery tests were conducted using the CM fortified with authentic 2(3*H*)-benzofuranone and azulene at three spiking concentrations (1, 10, and 100 μM) with five replicates. Controls and spiked samples were subjected to extraction and quantification using the method described above. Comparison of the standard deviation of the recoveries of five replicates on the same day for intra-day precision and analysis of spiked samples on three different days was determined for inter-day precision. Intra- and inter-day precision tests were both done at 1, 10, and 100 μM with nine replicates on three different days.

The linearity of calibration curves of 2(3*H*)-benzofuranone and azulene was 0.990 and 0.995, respectively, with the limit of

DOI: 10.1021/acs.est.9b04616
Environ. Sci. Technol. 2019, 53, 13042−13052

detection at 0.35 and 0.27 μM and the limit of quantification at 1.12 and 0.49 μM. Recovery tests showed that recoveries of the four compounds in various matrixes ranged over 79.9−95.7% with relative standard deviations of 4.4−12.0% (Table S6). Besides, the intra- and inter-day precision ranged over 5.6−10.8% at all spiked levels for the fortified samples tested.

RESULTS

Antagonistic Fungi Highly Enriched in the Asymptomatic Phyllosphere. From three paddy fields in Zhejiang province, we collected rice leaves with or without typical symptoms of *M. oryzae* infection and the culturable indigenous microbes were isolated from each sample based on distinguishable morphological characteristics. However, we observed that the number of rice leaf microbial isolates at different sampling positions showed no statistical difference between the asymptomatic and symptomatic phyllosphere (Figure 1A). Interestingly, the number of antagonistic fungal isolates from asymptomatic samples was significantly higher than that from symptomatic ones (Figure 1B). These observations suggest that the asymptomatic phenotype of rice leaves against *M. oryzae* is attributed to the relatively higher abundance of indigenous antagonistic fungal components in the phyllosphere.

***A. cvjetkovicii* as the Key Indigenous Fungus Responsible for the Asymptomatic Phyllosphere.** To identify the antagonistic microbes against *M. oryzae* that we obtained above, morphological observation was preliminarily carried out. Surprisingly, we noticed that several antagonistic isolates from the asymptomatic samples exerted remarkable inhibitory effect and similar morphological traits macroscopically. Colony diameters of the above similar antagonistic isolates ranged from 15 to 20 mm with abundant chartreuse conidia-secreted reddish brown pigment after 7 days of incubation on CMA at 25 °C in the dark (Figure S1). Combining with phylogenetic analysis of ribosomal ITS, we found that all these similar fungal isolates with identical ITS sequences were of the same strain, which belonged to the species *Aspergillus* (Figure S2).

Although ITS sequence of ribosome DNA was deemed as an available molecular marker for identification of fungi, it is not reliable in the case of *Aspergillus* spp. due to their high conservation and weak level of polymorphism among DNA sequences in the same genus.[45] Fortunately, *CaM* proposed as a secondary identification marker in *Aspergillus* spp.[45] was employed to identify these antagonistic fungal isolates. Consequently, all these morphologically identical fungal isolates are of 100% homology similarity of the *CaM* sequences with *A. cvjetkovicii* in the phylogenetic tree (Figure 2 and Table S7). Hence, these fungal isolates were accordingly assigned to be one strain *A. cvjetkovicii*.

Besides, qPCR analysis of *CaM* gene was employed to detect the relative abundance of *A. cvjetkovicii* in both asymptomatic and symptomatic phyllosphere. We observed that the abundance of *A. cvjetkovicii* in asymptomatic samples was 10-fold higher than that in the symptomatic ones ($p < 0.05$, Figure S3), which indicate that the significant difference of abundance of antagonistic *A. cvjetkovicii* in the microbial community composition is responsible for diverse phenotypes of the asymptomatic and symptomatic phyllosphere. We therefore hypothesized that the association of *A. cvjetkovicii* with the decrease of the incidence of *M. oryzae* was possibly mediated by the metabolic interaction in the phyllosphere.

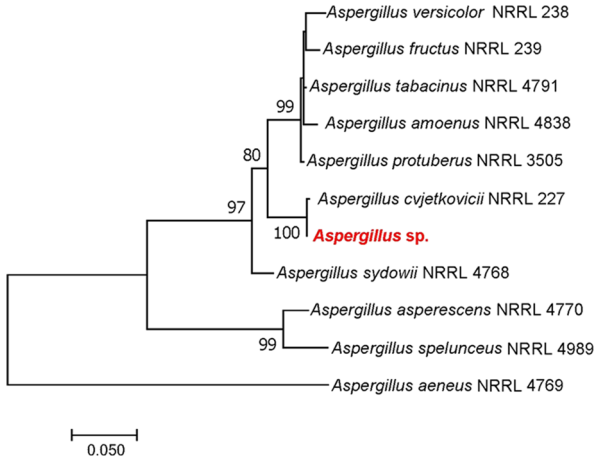

Figure 2. Maximum likelihood phylogenetic tree based on the *CaM* gene for identification of the dominant *Aspergillus* sp. in the rice phyllosphere. The number at the notes indicate the percentages of bootstrap sampling derived from 500 replications; values are shown only if greater than 75%. *Aspergillus aeneus* NRRL 4769 was used as an out-group. Bar, 0.05 substitutions per nucleotide position. Identity ranges from 98 to 100%.

Asymptomatic Metabolic Markers Positively Correlated with Indigenous *A. cvjetkovicii*. To determine the function of the phyllosphere indigenous microbe, *A. cvjetkovicii*, we visualized the characteristics and variation of the metabolites between asymptomatic and symptomatic leaves through GC-QqQ-MS/MS analysis. Several different compounds were detected between asymptomatic and symptomatic samples. Especially, the metabolites 1 and 2 were obviously detected in asymptomatic leaves but not enriched in symptomatic ones ($p < 0.05$, Figure 3A,B). This implies that these two metabolites as asymptomatic metabolic markers in the rice phyllosphere might be involved in the active interaction, leading to decreased incidence of *M. oryzae*.

Meanwhile, the simulating experiments were conducted to analyze whether the observed metabolic difference between the asymptomatic and symptomatic phyllosphere was linked with *A. cvjetkovicii*. Interestingly, we found that there were two metabolites increased remarkably in the asymptomatic phyllosphere when treated with conidia suspension of *A. cvjetkovicii* with a population-dependent manner (Figure 3C−F), whereas neither of them was detected in symptomatic leaves without the treatment of conidia suspension (Figure 3B). Furthermore, the rice blast disease incidences were decreased significantly with the increased population of conidia suspension of *A. cvjetkovicii* (Figure 4).

2(3*H*)-Benzofuranone and Azulene Identified as the Active Metabolites from *A. cvjetkovicii*. With the interest on the structure of these two metabolites produced by *A. cvjetkovicii* in the phyllosphere, further isolation and purification of the putative key metabolites and in vitro bioassay were conducted to investigate the impact of metabolites on *M. oryzae*. With comparison to Luria broth (LB), nutrition broth (NB), modified Winogradsky (MW), potato dextrose (PD), and complete medium (CM), CM was eventually selected due to the similar metabolic profile as shown in leaves and optimal mycelial growth for both *M. oryzae* and *A. cvjetkovicii*. Three liters of fermented broth of *A. cvjetkovicii* was extracted with ethyl acetate (EtOAc), leading to 0.760 g of soluble crude extracts. Twelve fractions were

DOI: 10.1021/acs.est.9b04616
Environ. Sci. Technol. 2019, 53, 13042−13052

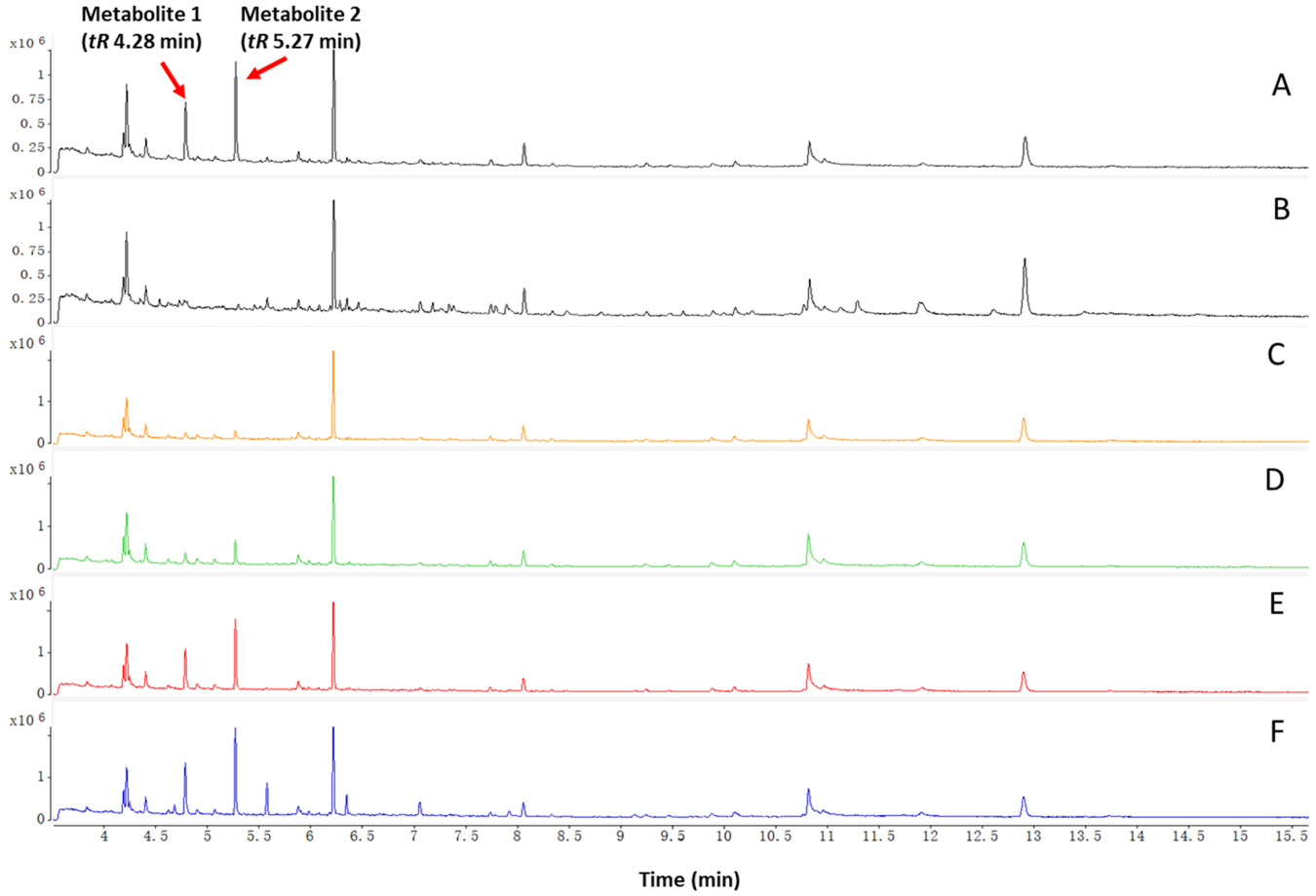

Figure 3. Metabolic profiling of rice phyllosphere samples. Differential metabolites detected at t_R of 4.28 and 5.27 min, respectively, were found to be accumulated exclusively in (A) asymptomatic phyllosphere but absent in (B) symptomatic one. (C−F) Profiling of two metabolites in the phyllosphere after being treated with *A. cvjetkovicii* at 10^2, 10^3, 10^4, and 10^5 conidia mL^{-1}, respectively. Spirodiclofen used as the internal standard was detected at 12.91 min.

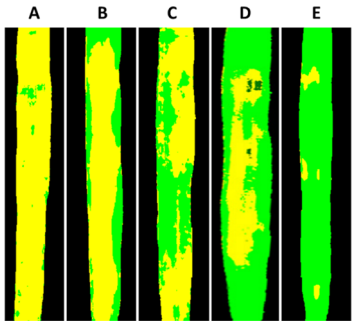

Figure 4. Visualization of disease incidence assay of the rice phyllosphere treated with gradient conidial suspensions of *A. cvjetkovicii*. (A−E) After being treated with *A. cvjetkovicii* at 0, 10^2, 10^3, 10^4, and 10^5 conidia mL^{-1}, respectively, development of symptoms of leaves was photographed after 5 days of inoculation.

collected by means of chromatography on silica gel and screened for their antimicrobial activity through the paper disk method (Figure S4). We observed that fraction 8 significantly suppressed the mycelial growth of *M. oryzae* by 86.94% and was of remarkable superiority to fractions 7 and 9 with inhibition rates of 69.29 and 62.57%, respectively (Table S1). Moreover, fraction 8 with the maximum inhibitory effect contained metabolites 1 and 2 simultaneously, while the fractions 7 and 9 with relatively lower inhibitory effects contained either metabolite 1 or 2 only (Figure 5A−C).

Subsequently, these two metabolites were purified and subjected to further structural characterization through GC-QqQ-MS/MS and NMR analyses. Comparing the spectral data of the sample compound with the reference spectra present in spectral libraries (NIST. 1), metabolite 1 showed an $[M]^+$ at *m/z* 134.0 ($C_8H_6O_2$) with two characteristic fragments at *m/z* 106.0 and 78.0 (Figure 5D), whereas metabolite 2 showed an $[M]^+$ at *m/z* 128.0 ($C_{10}H_8$) with two characteristic fragments at *m/z* 102.0 and 43.0 (Figure 5E). Besides, according to NMR spectral data, metabolites 1 and 2 were subsequently identified as 2(3*H*)-benzofuranone and azulene, respectively (Figure 5D,E, Figures S5−S8, and Tables S2 and S3), which were characterized as the active principles dominantly acted on the phyllosphere mediated the interaction between the indigenous *A. cvjetkovicii* and *M. oryzae*.

2(3*H*)-Benzofuranone and Azulene Temporally Affect the Morphogenesis Gene Expression in *M. oryzae*. For the further investigation of the mechanism mediated by 2(3*H*)-benzofuranone and azulene to disorder the development of *M. oryzae*, we preliminarily analyzed the production pattern of two metabolites by *A. cvjetkovicii* in a monoculture system. We found that 2(3*H*)-benzofuranone was first detected at the first day and reached the maximum level at the fifthday and maintained stability in the subsequent days (Figure 6A).

DOI: 10.1021/acs.est.9b04616
Environ. Sci. Technol. 2019, 53, 13042−13052

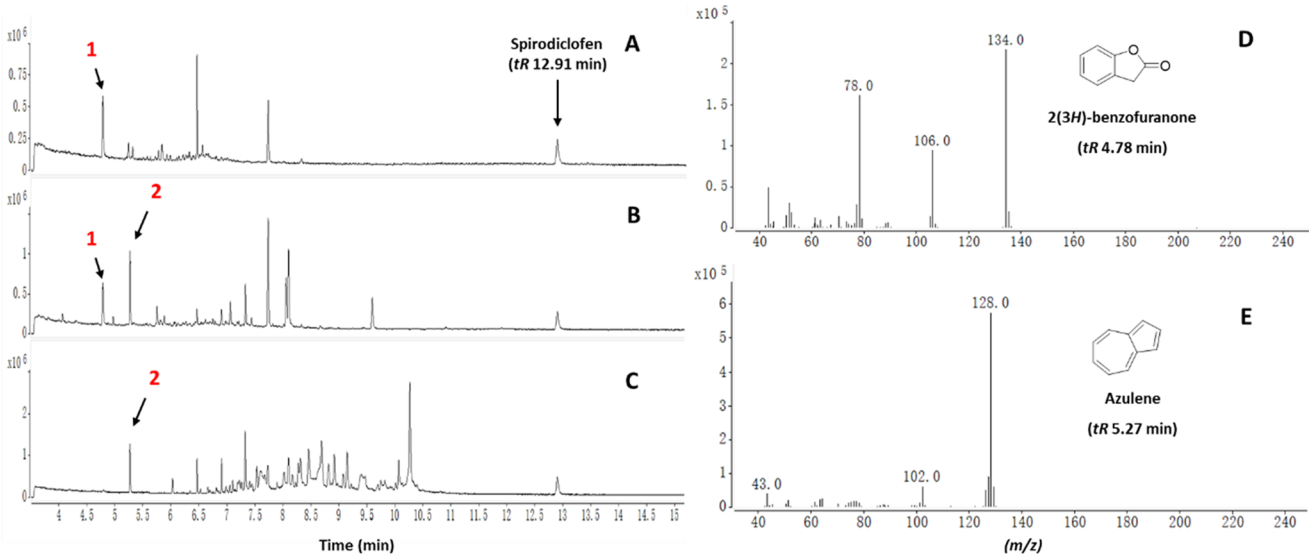

Figure 5. GC-QqQ-MS/MS analysis of metabolites 1 and 2 in active fractions of *A. cvjetkovicii* extracts. (B) Fraction 8 contained metabolites 1 and 2, simultaneously, while the fractions (A) 7 and (C) 9 contained either metabolite 1 or 2 only. (D) Metabolite 1 was detected at 4.28 min with characteristic fragments at *m/z* 134.0, 106.0, and 78.0. (E) Metabolite 2 was detected at 5.28 min with characteristic fragments at *m/z* 128.0, 102.0, and 43.0. Spirodiclofen used as the internal standard was detected at 12.91 min.

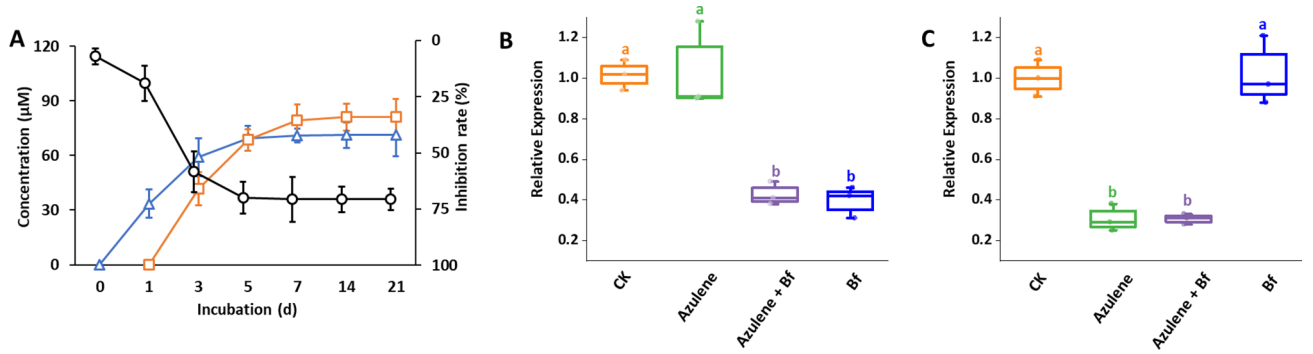

Figure 6. Analysis of accumulation dynamics and function of 2(3*H*)-benzofuranone and azulene in *A. cvjetkovicii*. Time course of 2(3*H*)-benzofuranone (blue) and azulene (orange) dynamics in culture media of *A. cvjetkovicii* and the inhibition rate (black) of extracts containing 2(3*H*)-benzofuranone and azulene on (A) *M. oryzae*. qRT-PCR assay of the expression of (B) *MoPer1* and (C) *MgRac1* (C) genes in *M. oryzae* treated with different combinations of 2(3*H*)-benzofuranone (Bf) and azulene. Values are means ± standard deviations (shown by error bars) of triplicates. Data with different letters are significantly different ($p < 0.01$).

However, azulene was initially detected at 3 days and peaked at 7 days, different from 2(3*H*)-benzofuranone. In addition, we observed that the inhibitory effect of 2(3*H*)-benzofuranone increased remarkably along with the time course and exhibited positive correlation with its accumulation (Figure 6A). Nevertheless, after 2(3*H*)-benzofuranone achieved the highest level, the inhibition rate was not enhanced due to increased accumulation of azulene despite reaching the maximum level. These results indicate that 2(3*H*)-benzofuranone and azulene are likely to affect the different stages in the morphogenesis of *M. oryzae*. Since 2(3*H*)-benzofuranone accumulated primarily at the early stage of *A. cvjetkovicii* and significantly inhibited the mycelial growth as the initial stage of rice blast disease, we hypothesize that the late-accumulated metabolite, azulene, mainly acted at the middle-late development period of *M. oryzae* accordingly suppressing disease epidemic.

To verify our hypothesis, the key morphogenesis-related gene expression model of different stages of rice blast development was analyzed. The results showed that the gene expression model of previously reported *MoPer1*, which is required for mycelial growth, marking the initial stage of *M. oryzae*, was quite different when treated with 2(3*H*)-benzofuranone, azulene, and both. We found that *MoPer1* was downregulated significantly when upon exposure to 2(3*H*)-benzofuranone or both compared to the controls ($p < 0.01$, Figure 6B). However, there were no statistical differences of *MoPer1* expression treated with the same concentration of azulene in comparison with the control group and neither between 2(3*H*)-benzofuranone and the mixture treatments. Our tests suggest that 2(3*H*)-benzofuranone, not azulene, involves in regulation of *MoPer1* expression, consequently inhibiting the predevelopment of *M. oryzae*. Moreover, the expression of gene *MgRac1* is of essential pathogenicity, and appressorium formation was detected for further function analysis of these two metabolites in the later stage of the development of *M. oryzae*. Surprisingly, the expression of *MgRac1* was slightly impacted by 2(3*H*)-benzofuranone (Figure 6C) but remarkably suppressed by azulene or the mixture with a similar effect, which is obviously different from *MoPer1* ($p < 0.01$, Figure 6B,C). Combining with the

DOI: 10.1021/acs.est.9b04616
Environ. Sci. Technol. 2019, 53, 13042−13052

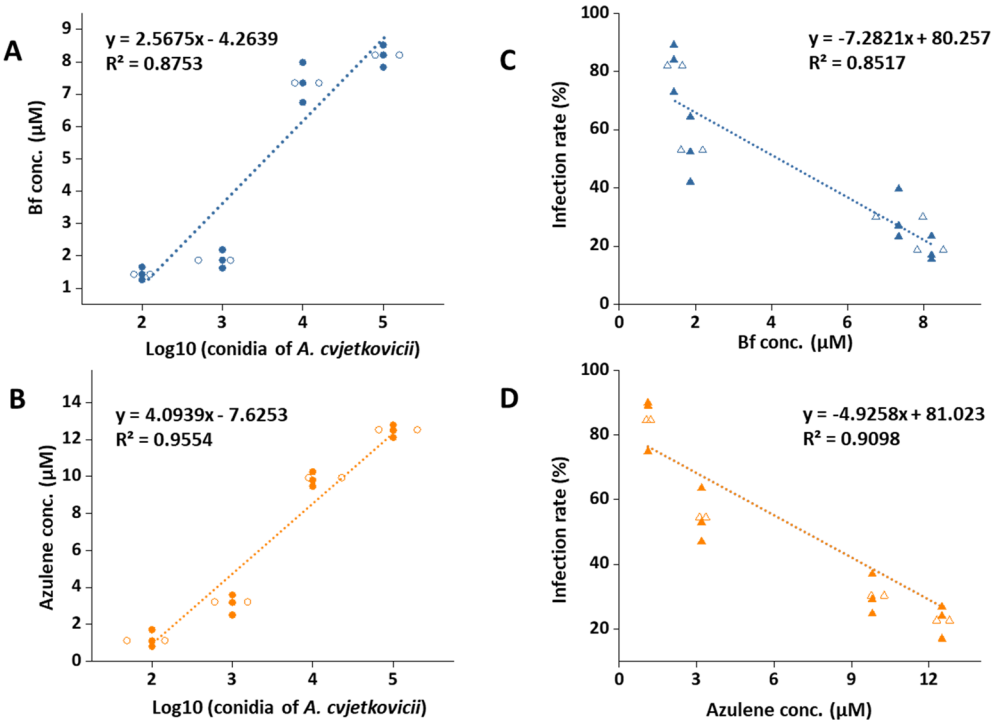

Figure 7. Relationship among conidia density, 2(3*H*)-benzofuranone and azulene production, and infection rate of *M. oryzae*. Conidia density corresponding to (A) 2(3*H*)-benzofuranone and (B) azulene productions was measured; correlation analysis of (C) 2(3*H*)-benzofuranone and (D) azulene concentrations and infection rate of *M. oryzae* were done using SPSS (version 20.0).

correlation analyses, the results indicate that the 2(3*H*)-benzofuranone and azulene were enriched showing a good linearity with the log 10 value of different conidia concentrations of *A. cvjetkovicii* (Figure 7A,B), giving linear equations: $y = 2.5675x - 4.2639$ ($R^2 = 0.8753$; $p < 0.01$) and $y = 4.0939x - 7.6253$ ($R^2 = 0.9554$, $p < 0.01$), respectively. Moreover, the disease incidence of *M. oryzae* was linearly negatively correlated with the accumulation of these two metabolites (Figure 7C,D), giving linear equations: $y = -7.2821x + 80.257$ ($R^2 = 0.8517$; $p < 0.01$) and $y = -4.9258x + 81.023$ ($R^2 = 0.9098$; $p < 0.01$), respectively. These observation results reconfirm our hypothesis and reveal that the metabolic interaction between *A. cvjetkovicii* and *M. oryzae* is in a time-dependent manner, and genes *MoPer1* and *MgRac1* involved in the signaling pathway and controlling the mycelial growth, pathogenicity, and appressorium formation of *M. oryzae* were regulated by these two active metabolites from *A. cvjetkovicii*, 2(3*H*)-benzofuranone and azulene, respectively.

DISCUSSION

The phyllosphere, the leaf surface-dominated microenvironment colonized by a wide array of microorganisms, makes up as an important above-ground fraction of phytobiome.[31,46,47] Compared with the more ecologically stable rhizosphere, this microenvironment experiences more dynamics in nutrient availability, is impacted by abiotic factors, and thus possesses a more distinct microbial composition.[46,48] However, similar to the biological interactions in the rhizosphere, these phyllosphere-inhabiting microbes encompass from competition to mutualism and impact fitness of the host plant, and are considered to have important functions for crop improvement programs.[32,49,50]

Interestingly, during the observation of phyllosphere culturable microbes between the asymptomatic and symptomatic rice leaves, we noticed an indigenous fungus (Figure 1), *A. cvjetkovicii*, which was exclusively enriched in the asymptomatic ones and capable of reducing *M. oryzae* infection remarkably. Although the toxin nonproducing *Aspergillus* spp. have been widely applied in biotechnological industries due to their extracellular secretions with antibiotic and enzymatic activities,[45] little is known about the roles of the *Aspergillus* in their hosts environmentally. Our current finding that an *A. cvjetkovicii*-mediated microecological response of rice to ward off the invasive *M. oryzae* reveals a novel ecological role of *A. cvjetkovicii* in the rice phyllosphere.

To sustain the microecological balance, the host plant has evolved ecologically diverse strategies, generally through release of self- and/or nonself-produced secondary metabolites to protect themselves from pathogen and herbivorous pests via the metabolic interaction.[51−53] With the further interest on metabolic interaction between *A. cvjetkovicii* and *M. oryzae* in situ, we observed the distinguishable metabolic profiles between the *A. cvjetkovicii*-detectable and nondetectable rice phyllosphere (Figure 3A,B) in which *A. cvjetkovicii* exerted a population-dependent manner to reduce *M. oryzae* infection incidence along with accumulation of 2(3*H*)-benzofuranone and azulene (Figure 3C−F). However, whether these two increased metabolites produced by *A. cvjetkovicii* or not was unclear. To address this issue, we obtained more information that there was no any detection of these two metabolites in the rice phyllosphere, but they were accumulated over time only when in the presence of *A. cvjetkovicii* (Figures 5 and 6A). These indicate that the ecological roles of *A. cvjetkovicii* in the phyllosphere are attributed to the productions of 2(3*H*)-benzofuranone and azulene to enhance host resistance to rice blast disease.

Previously, azulene was known to be derived from a variety of plants, including *Allium sativum* L., *Rosmarinus officinalis* L.,

DOI: 10.1021/acs.est.9b04616
Environ. Sci. Technol. 2019, 53, 13042−13052

and *Piper nigrum* L. as well as several endophytic fungi, such as *Muscodor* spp. and *Streptomyces alboflavus*.[54,55] Homoplastically, 2(3*H*)-benzofuranone is regarded as one natural product synthesized by diversified plants as well as microorganisms. So far, research has primarily focused on the pharmacology investigation of these two compounds, especially the therapeutic action on human beings. For example, azulene shows a marked anti-ulcerative effect and 2(3*H*)-benzofuranone can be prepared into an anti-inflammatory drug.[56,57] However, there were few reports about the antimicrobe functions of these two metabolites, and furthermore, their antimicrobial mechanisms were accordingly limited. In this work, both 2(3*H*)-benzofuranone and azulene could be biosynthesized by the indigenous fungus, *A. cvjetkovicii*, in the rice phyllosphere and involved in microbial interaction against *M. oryzae*.

During the following investigation of mode of action of these two metabolites on *M. oryzae*, we found that 2(3*H*)-benzofuranone remarkably inhibited the mycelial growth of *M. oryzae* supporting the diminution incidence of *M. oryzae* under the metabolite accumulation condition. However, to our surprise that azulene showed a little inhibitory effect on the development of *M. oryzae*, which did not conform to the reduction of the incidence rate when azulene was accumulated. Thus, we suggested that there might be a novel metabolite modulation model of *A. cvjetkovicii* against *M. oryzae* in the phyllosphere. Interestingly, the dynamic laws of 2(3*H*)-benzofuranone and azulene existed a time difference, leading to diverse prevention mechanisms from rice blast disease. As previously known, the genes of *MoPer1* and *MgRac1* are required for the mycelial growth and appressorium formation, respectively.[58,59] Thereinto, participation of *MoPer1* maintains the cell wall integrity, and disruption of *MoPer1* leads to a defect in morphological development in which the suppressed mycelial growth is responsible for the failure of *M. oryzae* invasion at the initial stage. However, *MgRac1* was regarded as the essential for the formation of appressorium and pathogenicity of *M. oryzae* via activating its downstream effector: the PKA kinase Chm1 and NADPH oxidases. Interestingly, the gene *MoPer1* in *M. oryzae* was significantly downregulated induced by 2(3*H*)-benzofuranone but not azulene. In contrast, the *MgRac1* was downregulated only when treating azulene. Based on the temporal spatial expression of the infection-related genes of *M. oryzae*, it was evidenced that these metabolites secreted at various times by *A. cvjetkovicii* disrupted the development of pathogen at different stages, and thus, a specific metabolite-mediated fungal interplay model in the rice phyllosphere under a temporal dependence manner was demonstrated. More importantly, phyllosphere application of either *A. cvjetkovicii* or 2(3*H*)-benzofuranone and azulene mixtures contributed to 63.6 and 54.7% significant reduction rates of *M. oryzae* epidemics in the air and 68.5 and 62.6% in the soil, respectively(Figure S9), which implying that this microenvironmental interplay plays a pivotal role in blocking epidemic cycles of *M. oryzae* in the paddy environment.

Taken together, our results revealed the implication of microenvironmental interplay dominated by indigenous and beneficial microbiota to ecological balance and safety of the paddy environment, and furthermore, this may shed light on the management of the fungal pathogen-associated biotoxin contamination in paddy and the surrounding natural environment.

■ ASSOCIATED CONTENT

Supporting Information

The Supporting Information is available free of charge on the ACS Publications website at DOI: 10.1021/acs.est.9b04616.

Figure S1, microscopy of conidia morphology of *A. cvjetkovicii*; Figure S2, neighbor-joining phylogenetic tree of the isolate *Aspergillus* sp. with 13 other fungal strains; Figure S3, enrichment of *A. cvjetkovicii* between the asymptomatic and symptomatic phyllosphere; Figure S4, flow chart of separation and purification of active metabolites of *A. cvjetkovicii*; Figure S5, ^{1}H NMR spectrum of metabolite 1; Figure S6, ^{13}C NMR spectrum of metabolite 1; Figure S7, ^{1}H NMR spectrum of metabolite 2; Figure S8, ^{13}C NMR spectrum of metabolite 2; Figure S9, epidemics of *M. oryzae* in the paddy environment; Table S1, single factor analysis of inhibitory effect of the fractions on mycelial growth of *M. oryzae;* Table S2, NMR spectroscopic analysis of metabolite 1 (2(3*H*)-benzofuranone); Table S3, NMR spectroscopic analysis of metabolite 2 (azulene); Table S4, primers and probe for PCR, qRT-PCR, and qPCR in this study; Table S5, key parameters for quantification of the *Aspergillus*-produced metabolites under MRM; Table S6, recovery test for 2(3*H*)-benzofuranone and azulene; Table S7, sequence of *CaM* gene of *A. cvjetkovicii* (PDF)

■ AUTHOR INFORMATION

Corresponding Author

*E-mail: wmctz@zju.edu.cn. Phone: +86-571-88982517. Fax: +86-571-88982517.

ORCID

Bartosz Nitkiewicz: 0000-0002-2821-5439

Qiangwei Wang: 0000-0001-5222-846X

Hua Fang: 0000-0002-3963-6175

Mengcen Wang: 0000-0001-7169-6779

Author Contributions

$^{\nabla}$These authors are equally contributed to this work.

Notes

The authors declare no competing financial interest.

■ ACKNOWLEDGMENTS

This work was supported by National Key R&D Program of China (2017YFE0102200 and 2017YFD0202100), Zhejiang Provincial Key Research and Development Program of China (2015C02019), National Natural Science Foundation of China (31501684), and Zhejiang Provincial Natural Science Foundation of China (LQ16C140001). We are also grateful to the local agricultural experiment stations for their assistance in field experiments and sampling.

■ REFERENCES

(1) Liu, X.; Fan, X.; Matsumoto, H.; Nie, Y.; Sha, Z.; Yi, K.; Pan, J.; Qian, Y.; Cao, M.; Wang, Y.; Zhu, G.; Wang, M. Biotoxin Tropolone Contamination Associated with Nationwide Occurrence of Pathogen *Burkholderia plantarii* in Agricultural Environments in China. *Environ. Sci. Technol.* **2018**, *52*, 5105−5114.

(2) Zhang, Q. Strategies for developing Green Super Rice. *Proc. Natl. Acad. Sci. U. S. A.* **2007**, *104*, 16402−16409.

(3) Wang, M.; Qian, Y.; Liu, X.; Wei, P.; Deng, M.; Wang, L.; Wu, H.; Zhu, G. Multiple spectroscopic analyses reveal the fate and metabolism of sulfamide herbicide triafamone in agricultural environments. *Environ. Pollut.* **2017**, *230*, 107−115.

(4) Ou, S. H. Pathogen Variability and Host Resistance in Rice Blast Disease. *Annu. Rev. Phytopathol.* **1980**, *18*, 167−187.
(5) Cheng, S.; Liu, H.; Sun, Q.; Kong, R.; Letcher, R. J.; Liu, C. Occurrence of the fungus mycotoxin, ustiloxin A, in surface waters of paddy fields in Enshi, Hubei, China, and toxicity in *Tetrahymena thermophila*. *Environ. Pollut.* **2019**, *251*, 901−909.
(6) Yun, C. S.; Motoyama, T.; Osada, H. Biosynthesis of the mycotoxin tenuazonic acid by a fungal NRPS-PKS hybrid enzyme. *Nat. Commun.* **2015**, *6*, 8758.
(7) Schenzel, J.; Forrer, H.-R.; Vogelgsang, S.; Hungerbühler, K.; Bucheli, T. D. Mycotoxins in the Environment: I. Production and Emission from an Agricultural Test Field. *Environ. Sci. Technol.* **2012**, *46*, 13067−13075.
(8) Bucheli, T. D. Phytotoxins: environmental micropollutants of concern? *Environ. Sci. Technol.* **2014**, *48*, 13027−13033.
(9) Dean, R.; Van Kan, J. A. L.; Pretorius, Z. A.; Hammond-Kosack, K. E.; Di Pietro, A.; Spanu, P. D.; Rudd, J. J.; Dickman, M.; Kahmann, R.; Ellis, J.; Foster, G. D. The Top 10 fungal pathogens in molecular plant pathology. *Mol. Plant. Pathol.* **2012**, *13*, 414−430.
(10) Jones, S. Magnaporthe blasts into roots. *Nat. Rev. Microbiol.* **2004**, *2*, 852−852.
(11) Gally, C.; Eimer, S.; Richmond, J. E.; Bessereau, J. L. A transmembrane protein required for acetylcholine receptor clustering in Caenorhabditis elegans. *Nature* **2004**, *431*, 578−582.
(12) Marcel, S.; Sawers, R.; Oakeley, E.; Angliker, H.; Paszkowski, U. Tissue-adapted invasion strategies of the rice blast fungus Magnaporthe oryzae. *Plant Cell* **2010**, *22*, 3177−3187.
(13) Osés-Ruiz, M.; Sakulkoo, W.; Littlejohn, G. R.; Martin-Urdiroz, M.; Talbot, N. J. Two independent S-phase checkpoints regulate appressorium-mediated plant infection by the rice blast fungus *Magnaporthe oryzae*. *Proc. Natl. Acad. Sci. U. S. A.* **2017**, *114*, e237−e244.
(14) Dean, R. A.; Talbot, N. J.; Ebbole, D. J.; Farman, M. L.; Mitchell, T. K.; Orbach, M. J.; Thon, M.; Kulkarni, R.; Xu, J.-R.; Pan, H.; et al. The genome sequence of the rice blast fungus *Magnaporthe grisea*. *Nature* **2005**, *434*, 980−986.
(15) Bonman, J. M. Durable resistance to rice blast disease-environmental influences. *Euphytica* **1992**, *63*, 115−123.
(16) Skamnioti, P.; Gurr, S. J. Against the grain: safeguarding rice from rice blast disease. *Trends Biotechnol.* **2009**, *27*, 141−150.
(17) de Jonge, R.; Ebert, M. K.; Huitt-Roehl, C. R.; Pal, P.; Suttle, J. C.; Spanner, R. E.; Neubauer, J. D.; Jurick, W. M., II; Stott, K. A.; Secor, G. A.; Thomma, B. P. H. J.; Van de Peer, Y.; Townsend, C. A.; Bolton, M. D. Gene cluster conservation provides insight into cercosporin biosynthesis and extends production to the genus *Colletotrichum*. *Proc. Natl. Acad. Sci. U. S. A.* **2018**, *115*, E5459−E5466.
(18) Kim, J.-C.; Min, J.-Y.; Kim, H.-T.; Cho, K.-Y.; Yu, S.-H. Pyricuol, a New Phytotoxin from *Magnaporthe grisea*. *Biosci., Biotechnol., Biochem.* **2014**, *62*, 173−174.
(19) Jiang, N.; Li, Z.; Wu, J.; Wang, Y.; Wu, L.; Wang, S.; Wang, D.; Wen, T.; Liang, Y.; Sun, P.; Liu, J.; Dai, L.; Wang, Z.; Wang, C.; Luo, M.; Liu, X.; Wang, G.-L. Molecular mapping of the Pi2/9 allelic gene Pi2-2 conferring broad-spectrum resistance to *Magnaporthe oryzae* in the rice cultivar Jefferson. *Rice* **2012**, *5*, 29.
(20) Ahn, S. W.; Ou, S. H. Quantitative resistance of rice to blast disease. *Phytopathology* **1982**, *72*, 279−282.
(21) Edwards, J.; Johnson, C.; Santos-Medellín, C.; Lurie, E.; Podishetty, N. K.; Bhatnagar, S.; Eisen, J. A.; Sundaresan, V. Structure, variation, and assembly of the root-associated microbiomes of rice. *Proc. Natl. Acad. Sci. U. S. A.* **2015**, *112*, E911−E920.
(22) Beckers, B.; De Beeck, M. O.; Weyens, N.; Boerjan, W.; Vangronsveld, J. Structural variability and niche differentiation in the rhizosphere and endosphere bacterial microbiome of field-grown poplar trees. *Microbiome* **2017**, *5*, 25.
(23) Konopka, A. What is microbial community ecology? *ISME J.* **2009**, *3*, 1223−1230.
(24) Berendsen, R. L.; Pieterse, C. M. J.; Bakker, P. A. H. M. The rhizosphere microbiome and plant health. *Trends Plant Sci.* **2012**, *17*, 478−486.
(25) Brader, G.; Compant, S.; Mitter, B.; Trognitz, F.; Sessitsch, A. Metabolic potential of endophytic bacteria. *Curr. Opin. Biotechnol.* **2014**, *27*, 30−37.
(26) Mendes, R.; Kruijt, M.; de Bruijn, I.; Dekkers, E.; van der Voort, M.; Schneider, J. H. M.; Piceno, Y. M.; DeSantis, T. Z.; Andersen, G. L.; Bakker, P. A. H. M.; Raaijmakers, J. M. Deciphering the Rhizosphere Microbiome for Disease-Suppressive Bacteria. *Science* **2011**, *332*, 1097−6100.
(27) Yong, Y.-C.; Wu, X.-Y.; Sun, J.-Z.; Cao, Y.-X.; Song, H. Engineering quorum sensing signaling of *Pseudomonas* for enhanced wastewater treatment and electricity harvest: A review. *Chemosphere* **2015**, *140*, 18−25.
(28) Guttman, D. S.; McHardy, A. C.; Schulze-Lefert, P. Microbial genome-enabled insights into plant-microorganism interactions. *Nat. Rev. Genet.* **2014**, *15*, 797−813.
(29) DeAngelis, K. M.; Brodie, E. L.; DeSantis, T. Z.; Andersen, G. L.; Lindow, S. E.; Firestone, M. K. Selective progressive response of soil microbial community to wild oat roots. *ISME J.* **2009**, *3*, 168−178.
(30) Mendes, L. W.; Raaijmakers, J. M.; de Hollander, M.; Mendes, R.; Tsai, S. M. Influence of resistance breeding in common bean on rhizosphere microbiome composition and function. *ISME J.* **2018**, *12*, 212−224.
(31) Vorholt, J. A. Microbial life in the phyllosphere. *Nat. Rev. Microbiol.* **2012**, *10*, 828−840. Coca, M.; Bortolotti, C.; Rufat, M.; Peñas, G.; Eritja, R.; Tharreau, D.; Del Pozo, A. M.; Messeguer, J.; San Segundo, B. Transgenic rice plants expressing the antifungal AFP protein from *Aspergillus giganteus* show enhanced resistance to the rice blast fungus *Magnaporthe grisea*. *Plant Mol. Biol.* **2004**, *54*, 245−259.
(32) Wang, M.; Hashimoto, M.; Hashidoko, Y. Carot-4-en-9,10-diol, a conidiation-inducing sesquiterpene diol produced by *Trichoderma virens* PS1-7 upon exposure to chemical stress from highly active iron chelators. *Appl. Environ. Microbiol.* **2013**, *79*, 1906−1914.
(33) Matar, K. A. O.; Chen, X.; Chen, D.; Anjago, W. M.; Norvienyeku, J.; Lin, Y.; Chen, M.; Wang, Z.; Ebbole, D. J.; Lu, G.-d. WD40-repeat protein MoCreC is essential for carbon repression and is involved in conidiation, growth and pathogenicity of *Magnaporthe oryzae*. *Curr. Genet.* **2017**, *63*, 685−696.
(34) Matheis, S.; Yemelin, A.; Scheps, D.; Andresen, K.; Jacob, S.; Thines, E.; Foster, A. J. Functions of the *Magnaporthe oryzae* Flb3p and Flb4p transcription factors in the regulation of conidiation. *Microbiol. Res.* **2017**, *196*, 106.
(35) Moreno, A. B.; del Pozo, Á. M.; San Segundo, B. Biotechnologically relevant enzymes and proteins. Antifungal mechanism of the Aspergillus giganteus AFP against the rice blast fungus *Magnaporthe grisea*. *Appl. Microbiol. Biotechnol.* **2006**, *72*, 883−895.
(36) Chen, Y.; Zhu, J.; Ying, S. H.; Feng, M. G. Three Mitogen-Activated Protein Kinases Required for Cell Wall Integrity Contribute Greatly to Biocontrol Potential of a Fungal *Entomopathogen*. *PLoS One* **2014**, *9*, No. e87948.
(37) Ritpitakphong, U.; Falquet, L.; Vimoltust, A.; Berger, A.; Métraux, J. P.; L'Haridon, F. The microbiome of the leaf surface of *Arabidopsis* protects against a fungal pathogen. *New Phytol.* **2016**, *210*, 1033−1043.
(38) Yergeau, E.; Hogues, H.; Whyte, L. G.; Greer, C. W. The functional potential of high Arctic permafrost revealed by metagenomic sequencing, qPCR and microarray analyses. *ISME J.* **2010**, *4*, 1206−1214.
(39) Zheng, W.; Chen, J.; Liu, W.; Zheng, S.; Zhou, J.; Lu, G.; Wang, Z. A Rho3 homolog is essential for appressorium development and pathogenicity of *Magnaporthe grisea*. *Eukaryotic Cell* **2007**, *6*, 2240−2250.
(40) Otsu, N. A Threshold Selection Method from Gray-Level Histograms. *IEEE Trans. Syst., Man, Cybern.* **1979**, *9*, 62−66.

DOI: 10.1021/acs.est.9b04616
Environ. Sci. Technol. 2019, 53, 13042−13052

(41) Cao, M.; Li, S.; Wang, Q.; Wei, P.; Liu, Y.; Zhu, G.; Wang, M. Track of fate and primary metabolism of trifloxystrobin in rice paddy ecosystem. *Sci. Total Environ.* **2015**, *518-519*, 417−423.
(42) Livak, K. J.; Schmittgen, T. D. Analysis of relative gene expression data using real-time quantitative PCR and the $2^{-\Delta\Delta C_T}$ Method. *Methods* **2001**, *25*, 402−408.
(43) Xue, L. Y.; Zhao, L. W.; Hu, Y. F.; Qiu, H. P.; Chai, R. Y.; Zhang, Z. Development of a qPCR detection method for monitoring conidial density of rice blast fungus in the air. *Acat Agric. Zhejiangensis* **2016**, *28*, 1368−1373. (in Chinese)
(44) Su'udi, M.; Kim, J.; Park, J.-M.; Bae, S.-C.; Kim, D.; Kim, Y.-H.; Ahn, I.-P. Quantification of Rice Blast Disease Progressions Through Taqman Real-Time PCR. *Mol. Biotechnol.* **2013**, *55*, 43−48.
(45) Samson, R. A.; Visagie, C. M.; Houbraken, J.; Hong, S.-B.; Hubka, V.; Klaassen, C. H. W.; Perrone, G.; Seifert, K. A.; Susca, A.; Tanney, J. B.; Varga, J.; Kocsubé, S.; Szigeti, G.; Yaguchi, T.; Frisvad, J. C. Phylogeny, identification and nomenclature of the genus *Aspergillus*. *Stud. Mycol.* **2014**, *78*, 141−173.
(46) Leach, J. E.; Triplett, L. R.; Argueso, C. T.; Trivedi, P. Communication in the Phytobiome. *Cell* **2017**, *169*, 587−596.
(47) Beans, C. Core Concept: Probing the phytobiome to advance agriculture. *Proc. Natl. Acad. Sci. U. S. A.* **2017**, *114*, 8900−8902.
(48) Parakhia, M. V. Manipulation of phytobiome: a new concept to control the plant disease and improve the productivity. *J. Bacteriol. Mycol.: Open Access* **2018**, *6*, 322−324.
(49) Rybakova, D.; Mancinelli, R.; Wikström, M.; Birch-Jensen, A. S.; Postma, J.; Ehlers, R.-U.; Goertz, S.; Berg, G. The structure of the Brassica napus seed microbiome is cultivar-dependent and affects the interactions of symbionts and pathogens. *Microbiome* **2017**, *5*, 104.
(50) van der Heijden, M. G. A.; Hartmann, M. Networking in the Plant Microbiome. *PLoS Biol.* **2016**, *14*, No. e1002378.
(51) Evangelisti, E.; Rey, T.; Schornack, S. Cross-interference of plant development and plant−microbe interactions. *Curr. Opin. Plant Biol.* **2014**, *20*, 118−126.
(52) Shikano, I.; Rosa, C.; Tan, C. W.; Felton, G. W. Tritrophic Interactions: Microbe-Mediated Plant Effects on Insect Herbivores. *Annu. Rev. Phytopathol.* **2017**, *55*, 313−331.
(53) Bais, H. P.; Weir, T. L.; Perry, L. G.; Gilroy, S.; Vivanco, J. M. The role of root exudates in rhizosphere interactions with plants and other organisms. *Annu. Rev. Plant Biol.* **2006**, *57*, 233−266.
(54) Yang, M.; Lu, L.; Pang, J.; Hu, Y.; Guo, Q.; Li, Z.; Wu, S.; Liu, H.; Wang, C. Biocontrol activity of volatile organic compounds from *Streptomyces alboflavus* TD-1 against *Aspergillus flavus* growth and aflatoxin production. *J. Microbiol.* **2019**, *57*, 396−404.
(55) Mitchell, A. M.; Strobel, G. A.; Moore, E.; Robison, R.; Sears, J. Volatile antimicrobials from *Muscodor crispans, a novel endophytic fungus*. *Microbiology* **2009**, *156*, 270−277.
(56) Lysenko, L. V. Anti-inflammatory effect of azulene of eucalyptus oil. *Farmakol Toksikol* **1967**, *30*, 341−343.
(57) de Souza Nunes, J. P.; da Silva, K. A. B.; da Silva, G. F.; Quintão, N. L. M.; Corrêa, R.; Cechinel-Filho, V.; de Campos-Buzzi, F.; Niero, R. The antihypersensitive and antiinflammatory activities of a benzofuranone derivative in different experimental models in mice: the importance of the protein kinase C pathway. *Anesth. Analg.* **2014**, *119*, 836−846.
(58) Chen, J.; Zheng, W.; Zheng, S.; Zhang, D.; Sang, W.; Chen, X.; Li, G.; Lu, G.; Wang, Z. *Rac1* is required for pathogenicity and *Chm1*-dependent conidiogenesis in rice fungal pathogen *Magnaporthe grisea*. *PLoS Pathog.* **2008**, *4*, No. e1000202.
(59) Chen, Y.; Wu, X.; Li, C.; Zeng, Y.; Tan, X.; Zhang, D.; Liu, Y. MoPer1 is required for growth, conidiogenesis, *and pathogenicity in Magnaporthe oryzae*. *Rice* **2018**, *11*, 64.

DOI: 10.1021/acs.est.9b04616
Environ. Sci. Technol. 2019, 53, 13042−13052